

Electronic Supplementary Information

A Scalable Aluminum Niobate Anode for High Energy, High Power Practical Lithium-Ion Batteries

Matthew W. Logan*, Dajie Zhang, Bing Tan, and Konstantinos Gerasopoulos*

Research and Exploratory Development Department, Johns Hopkins University Applied Physics Laboratory, 11000 Johns Hopkins Rd, Laurel, MD, 20273

*corresponding authors: matthew.logan@jhuapl.edu and konstantinos.gerasopoulos@jhuapl.edu

Supporting Figures

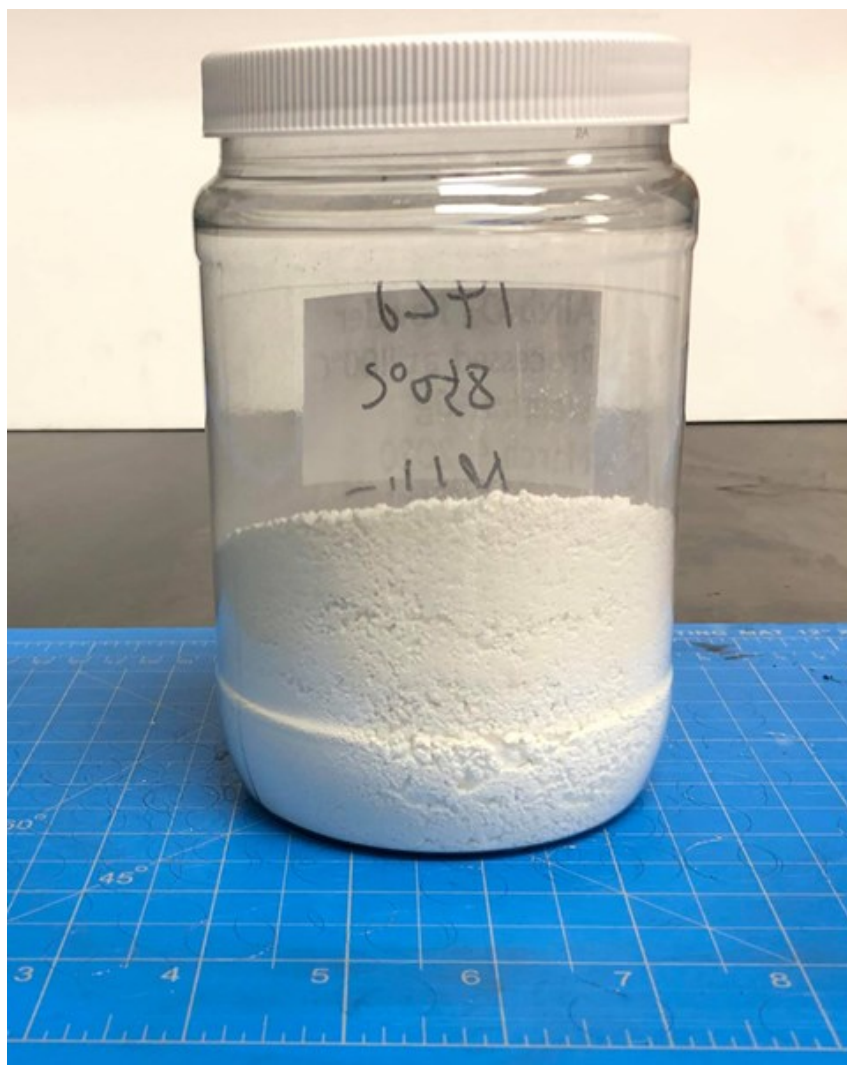


Figure S1: 140 g batch production of ANO powder.

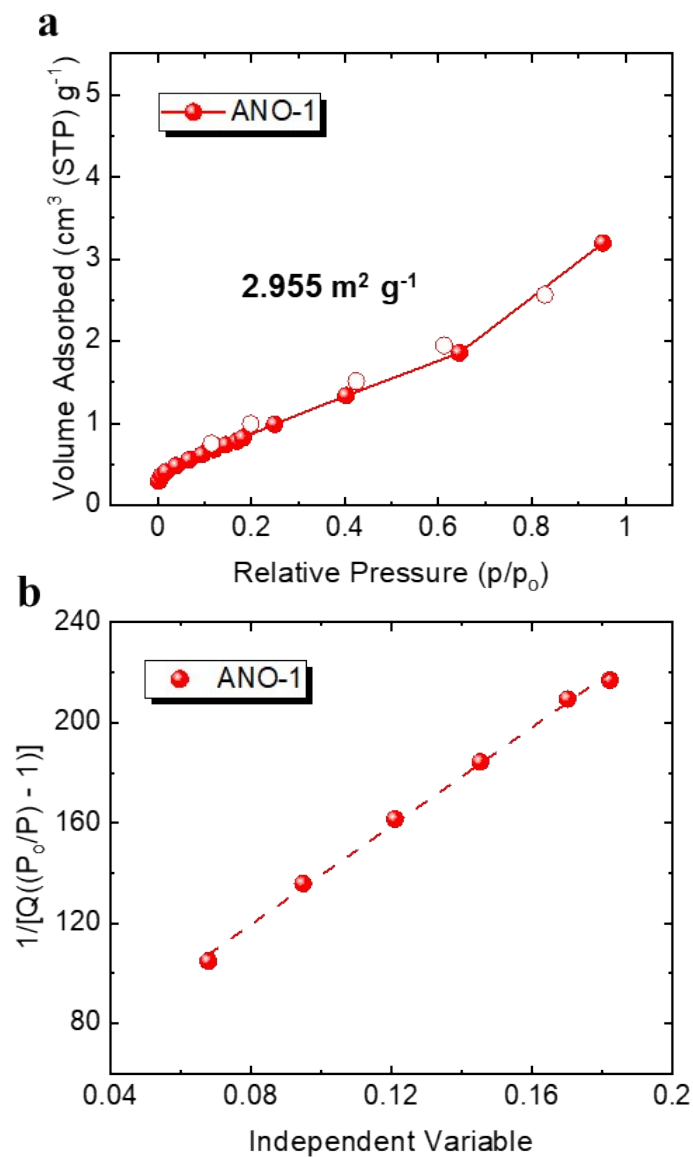


Figure S2: Nitrogen gas sorption isotherm (77 K, $p_0 = 760$ torr) for ANO. Closed circles represent adsorption and open circles, desorption. (b) Linear fitting curve for BET analysis of the accessible surface area for ANO. Experimental results are shown as solids spheres, fitting as a dashed line.

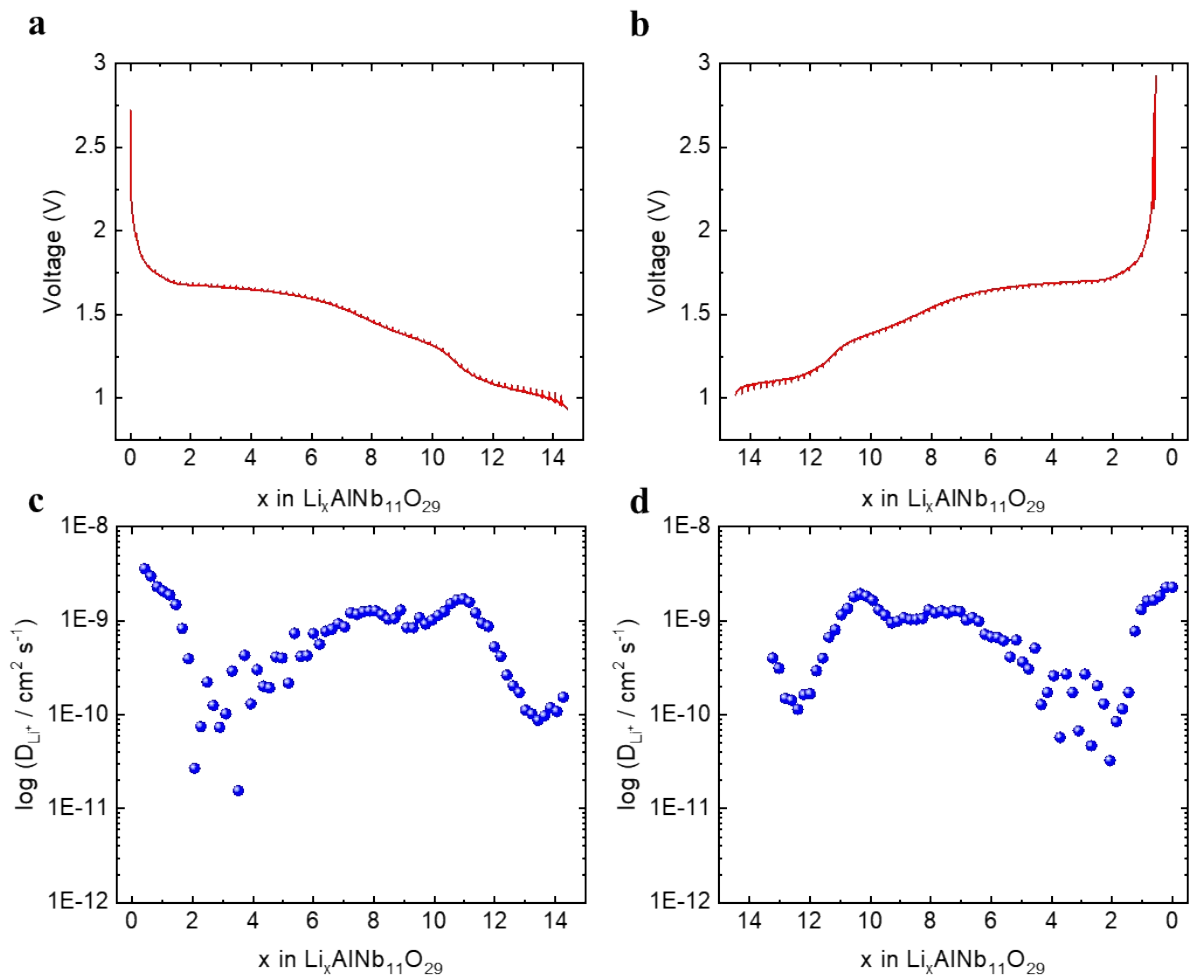


Figure S3: Galvanostatic intermittent titration technique (GITT) experiments of ANO/Li half cells during (a) lithiation and (b) delithiation. Cells were pulsed at $C/10$ over 600 s followed by a relaxation step at open circuit for 1200 s at room temperature. The D_{Li} coefficients values for (c) lithiation and (d) delithiation were determined from GITT measurement.

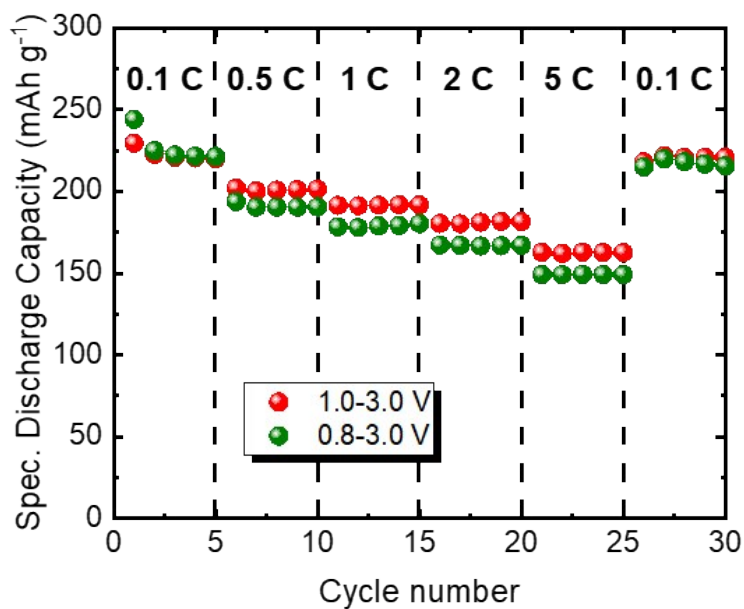


Figure S4: Rate-performance properties for ANO-1/Li half cells evaluated between different discharge cutoff potentials. Cutoff voltages of 1.0–3.0 V and 0.8–3.0 V vs. Li/Li⁺ were used with cells cycled from 0.1–5 C in five cycle increments. The capacity values were normalized to the active mass of the respective electrode.

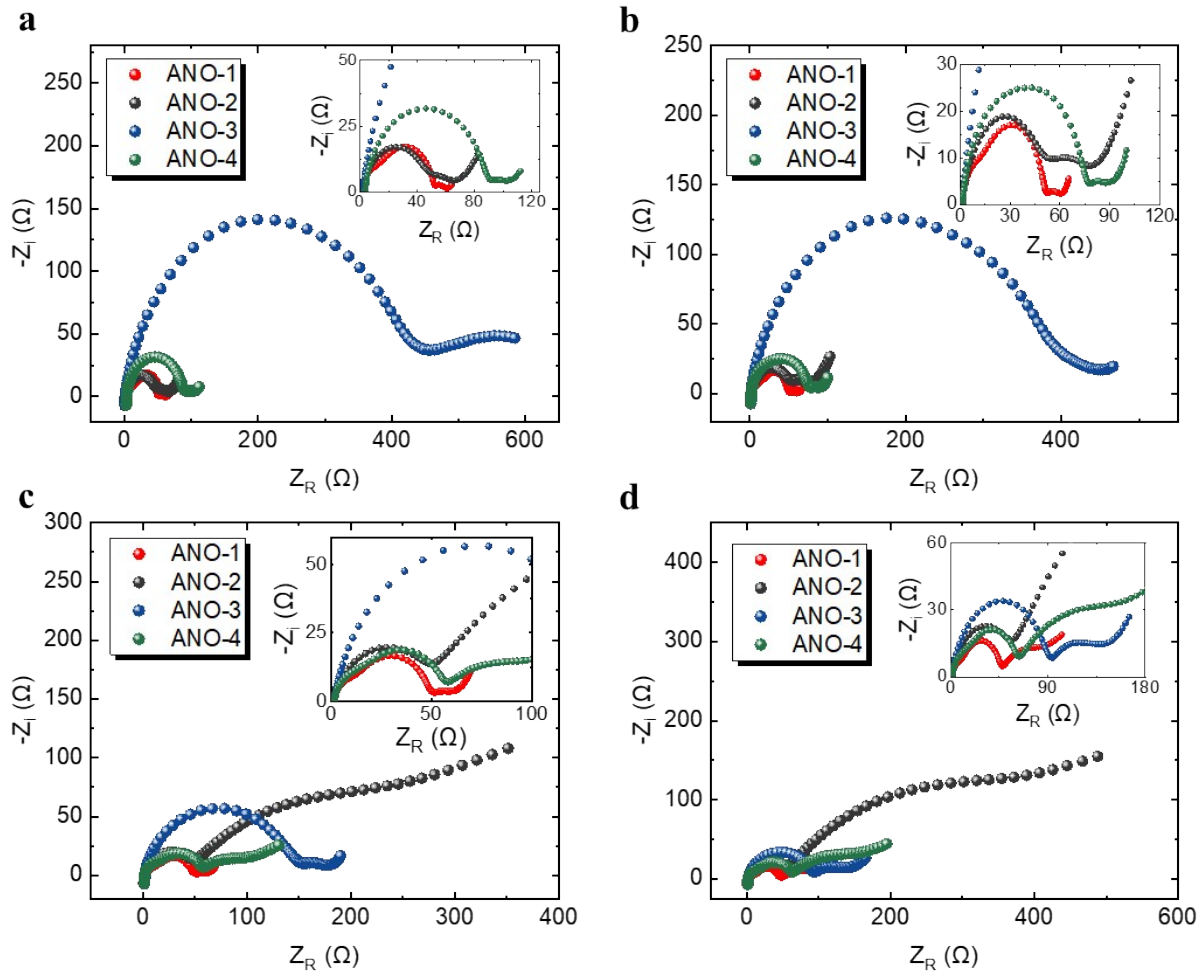


Figure S5: Nyquist plots at (a) 25%, (b) 50%, (c) 75%, and (d) 100% SOC of ANO-1, ANO-2, ANO-3, ANO-4, and LTO-1. EIS measurements were recorded in a frequency range of 10^5 – 10^{-2} Hz.

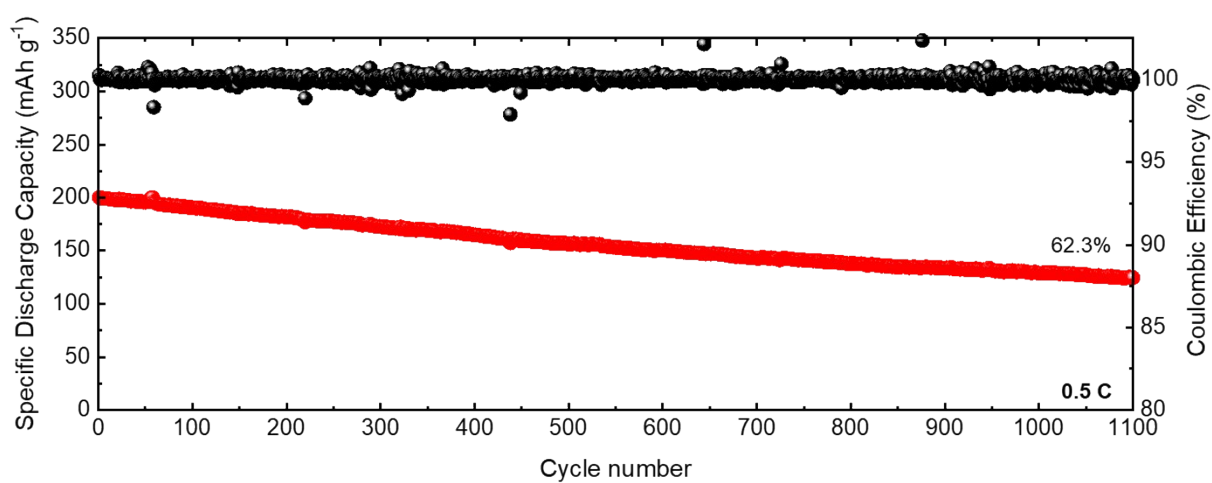


Figure S6: Long-term cycle stability of ANO-1 electrode at 0.5 C with corresponding Coulombic Efficiency on the secondary y-axis. Cutoff voltages of 1.0 and 3.0 V vs. Li/Li⁺ were used with capacity values normalized to the active mass of ANO-1. Specific discharge capacity shown in solid red circles with Coulombic efficiency shown in solid black circles.

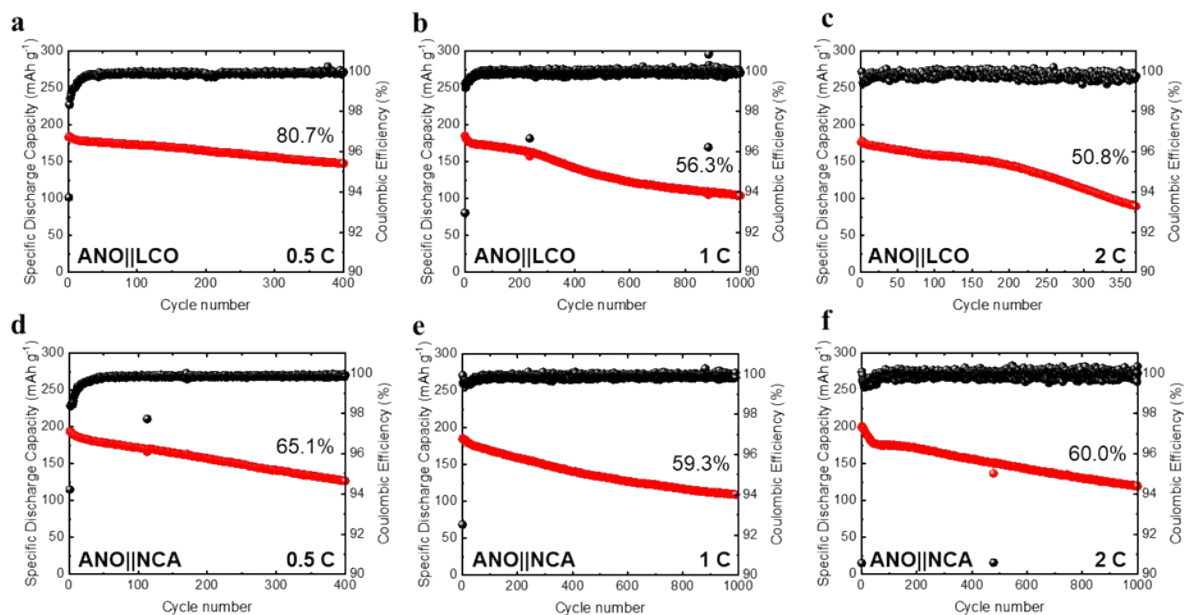


Figure S7: Electrochemical properties of ANO full cells with a N/P ratio of 0.9 (2.17:2.4 mAh cm⁻²). Cycle performance of ANO||LCO cells cycled at (a) 0.5 C, (b) 1 C, and (c) 2 C. ANO||NCA cells cycled at (d) 0.5 C, (e) 1 C, and (f) 2 C. Capacity values were normalized to the total active mass of ANO. Specific discharge capacity shown in solid red circles with Coulombic efficiency shown in solid black circles. The % of capacity retention is also shown in the graphs.

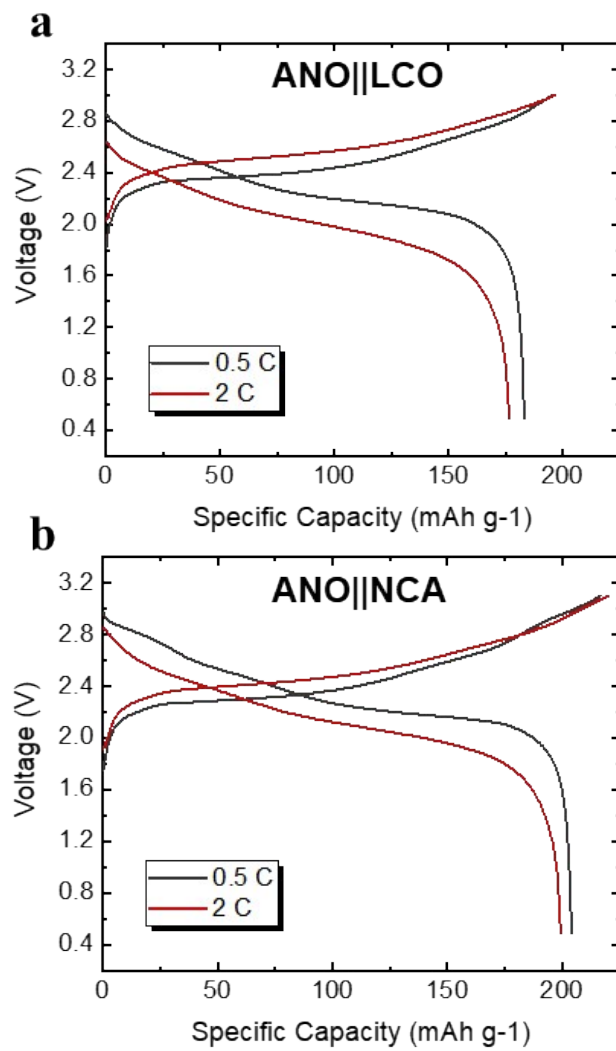


Figure S8: First cycle charge-discharge curves of (a) ANO||LCO and (b) ANO||NCA full cells at 0.5 C and 2 C.

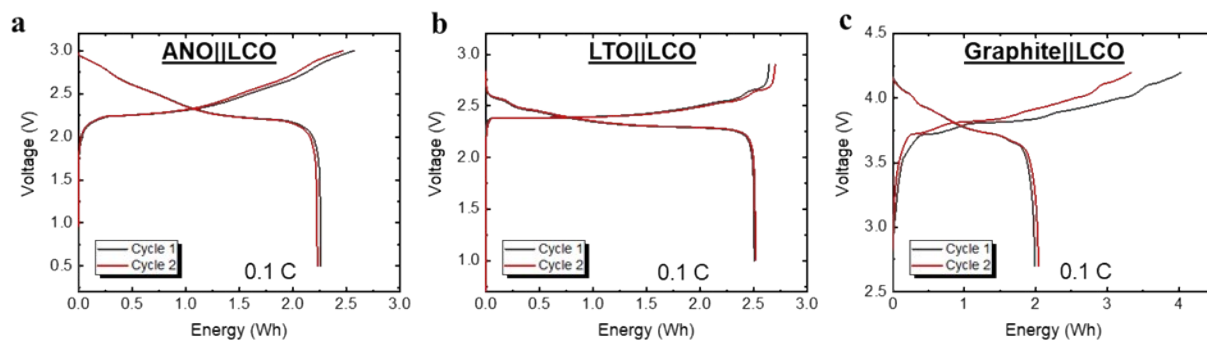


Figure S9: Galvanostatic charge-discharge curves of 2.5 Wh full cells (a) ANO||LCO, (b) LTO||LCO, and (c) graphite||LCO. Cells were constructed with 25 μm polypropylene separators and cycled at 0.1 C.

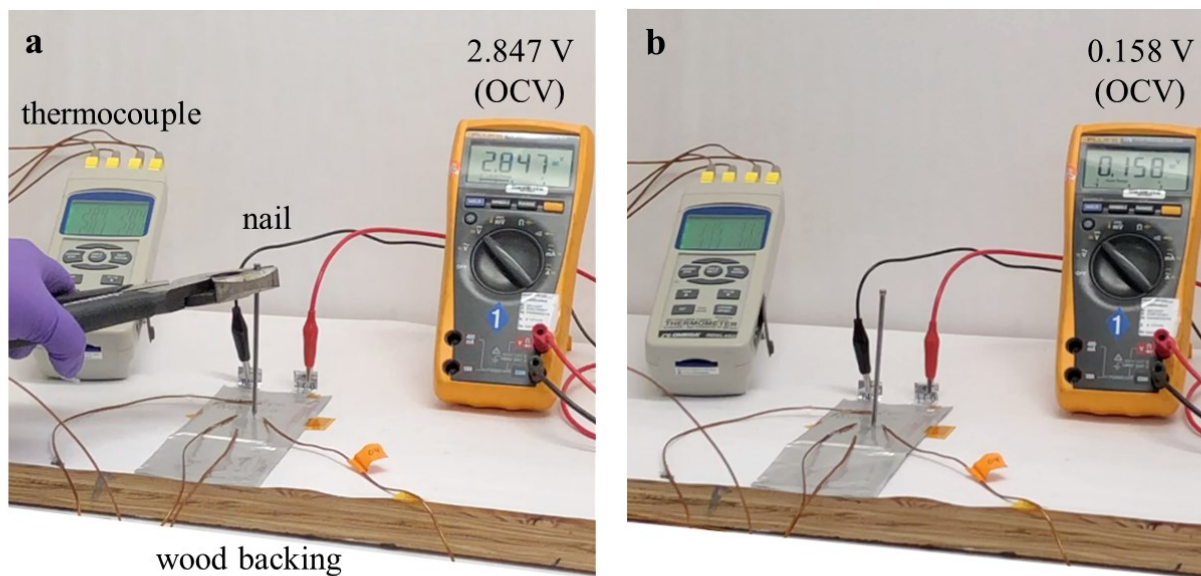


Figure S10: Optical image of (a) 2.5 Wh ANO||LCO (GF/C) cell before (at open-circuit voltage (OCV)) and (b) after nail penetration (verifying electrical short).

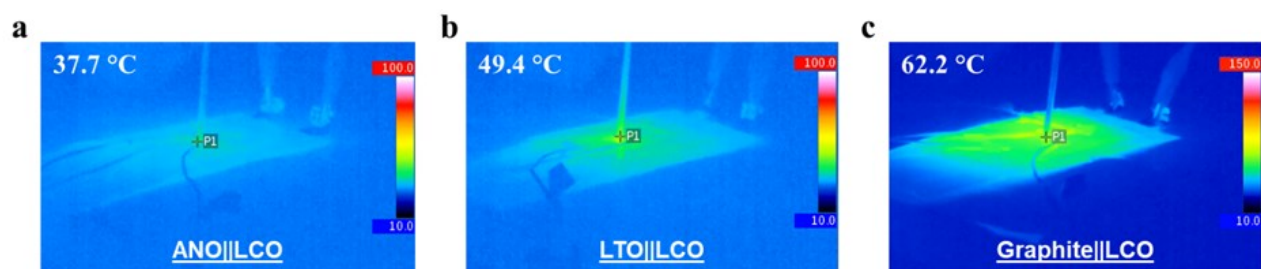


Figure S11: Nail penetration performed on 2.5 Wh full cells with 25 μm polypropylene separator showing the highest temperature recorded through the duration of the experiment.

Supporting Tables

Table S1: Theoretical numerical values used to calculate the volumetric capacities shown in Figure 1. Porosity is assumed to be 30% for all electrodes with an areal capacity of 2.0 mAh cm^{-2} .

Anode Material	Active Material (wt%)	C65 (wt%)	PVDF (wt%)	Theo. Cap. (mAh g ⁻¹) ^a	Avg. Density (g cm ⁻³) ^b	Areal Mass loading (mg cm ⁻²)	Thickness (μm) ^c	Vol. Cap. (mAh cm ⁻³) ^d
Graphite	95	0	5	372	2.23	5.66	36.26	551
LTO	90	5	5	175	3.19	12.70	56.78	352
ANO	90	5	5	390	3.52	5.70	23.12	865

^aTheoretical capacity based on the active material. ^bAverage density is calculated from the C65, PVDF, and skeletal density derived from corresponding Crystallographic Information File (CIF). ^cThickness calculated without a current collector. ^dVolumetric capacity calculated without a current collector.

Table S2: Results of the crystal structure analysis by Rietveld refinement of as-synthesized ANO.

a (Å)	b (Å)	c (Å)	α, γ (°)	β (°)	V (nm ³)	Rwp
15.561248(67)	3.812895(16)	20.232341(82)	90	113.043(4)	1.104652(132)	0.0969

Table S3: Fractional atomic parameters of as-synthesized ANO.

Atom ^a	symmetry	site	x	y	z
M1	<i>m</i>	4 <i>i</i>	0.3661	0	0.7793
M2	<i>m</i>	4 <i>i</i>	0.0970	0	0.8814
M3	<i>m</i>	4 <i>i</i>	0.3659	0	0.9638
M4	<i>m</i>	4 <i>i</i>	0.3668	0	0.1492
M5	<i>m</i>	4 <i>i</i>	0.0962	0	0.6969
M6	<i>m</i>	4 <i>i</i>	0.0987	0	0.0680
O1	2/ <i>m</i>	2 <i>d</i>	0.5000	0.5000	0.5000
O2	<i>m</i>	4 <i>i</i>	0.3643	0	0.4627
O3	<i>m</i>	4 <i>i</i>	0.2277	0	0.729
O4	<i>m</i>	4 <i>i</i>	0.3643	0	0.2471
O5	<i>m</i>	4 <i>i</i>	0.2204	0	0.1063
O6	<i>m</i>	4 <i>i</i>	0.2219	0	0.9218
O7	<i>m</i>	4 <i>i</i>	0.0381	0	0.3578
O8	<i>m</i>	4 <i>i</i>	0.0900	0	0.7838
O9	<i>m</i>	4 <i>i</i>	0.3638	0	0.8690
O10	<i>m</i>	4 <i>i</i>	0.0862	0	0.6021
O11	<i>m</i>	4 <i>i</i>	0.3623	0	0.0553
O12	<i>m</i>	4 <i>i</i>	0.3640	0	0.6777
O13	<i>m</i>	4 <i>i</i>	0.0741	0	0.9709
O14	<i>m</i>	4 <i>i</i>	0.5000	0	0.1882
O15	<i>m</i>	4 <i>i</i>	0.0658	0	0.16650

$$^aM = 11/12 Nb^{5+} + 1/12 Al^{3+}$$

Table S4: Fully charged anode ambient reactivity test results.

Trial	ANO Temperature (°C)	LTO Temperature (°C)	Graphite Temperature (°C)
1	239.9	244.2	57.9
2	259.3	256.3	55.6
3	297.2	223.0	58.9
4	236.9	222.3	52.7
Average	258.3	250.3	56.3